High Resolution Positive Contrast Imaging: Application to the Visualization of Localized Vascular Abnormalities

T. G. Perkins[1], J. Sénégas[2], H. Dahnke[2], E. Sandberg[3,4], and W. W. Orrison[5,6]

[1]Philips Healthcare, Cleveland, OH, United States, [2]Philips Research Europe, Hamburg, Germany, [3]Department of Radiology, VAMC, Denver, CO, United States, [4]Departments of Radiology and Neurology, University of Colorado Health Science Center, Aurora, CO, United States, [5]Nevada Imaging Centers, Las Vegas, NV, United States, [6]Touro University Nevada College of Osteopathic Medicine, Henderson, NV, United States

Introduction Positive contrast imaging [1, 2] based on susceptibility gradient mapping (SGM) is a relatively new technique that produces maps with high contrast-to-noise ratio for areas of local magnetic susceptibility variation [3, 4]. Recent work has focused on increasing the resolution of such maps, which has enhanced the ability to detect super paramagnetic iron oxide (SPIO) particles within labeled cells and to impart positive contrast on vessels in the brain at 7T [5]. Applying high resolution SGM to assess localized abnormalities associated with hemosiderin deposition in conditions such as traumatic brain injury or cavernous angiomas could provide additional clinical information for detection and diagnosis. The purpose of this study was to explore the potential clinical utility of SGM to provide better characterization of cavernous angiomas.

Materials and Methods Positive contrast images were obtained from data collected at 1.5T and 3T using clinical Achieva MR systems (Philips Healthcare, Best, The Netherlands) and eight-channel SENSE head coils. A 3D gradient echo sequence whose parameters were optimized for each field strength was applied for data acquisition. At 1.5T, a 3D Principles of Echo Shifting with a Train of Observations (PRESTO) sequence was used with a TR/TE of 20/26 ms, a flip angle of 7°, a slice thickness of 1.8 mm (0.0 mm gap), a 240 mm FOV with 0.9 mm in-plane resolution, 85 slices, and an acquisition time of 3min 30 sec. At 3T, a 3D Fast Field Echo (FFE) sequence was used with a TR/TE of 19/12 ms, a flip angle of 10°, a slice thickness of 0.9 mm (0.0 mm gap), a 230 mm FOV with 0.9 mm in-plane resolution, 150 slices, and an acquisition time of 4min 58 sec. For both protocols, modulus, real, and imaginary images were reconstructed. Positive contrast images were generated from the real and imaginary datasets using both the standard SGM method [4] and the recently proposed high resolution SGM method [5] for comparative purposes.

Results Figure 1 shows a midbrain axial slice from a patient with multiple cavernous angiomas obtained at 1.5T. The modulus of the gradient echo image is displayed in Fig. 1a, while Fig. 1b and 1c show the corresponding low resolution and high resolution SGM maps. The gradient echo image, while presenting the usual hypointense signal associated with the cavernous angiomas, provides little, if any, structural or anatomical detail within these regions. The low resolution positive contrast image shows hyperintense signal within and around the angiomas, indicating that these are associated with increased local magnetic susceptibility. The high resolution positive contrast image additionally shows internal structure within the lesions that can be related to the vascular structure of the angiomas. Note the excellent visualization of the tissue boundary between the putamen and surrounding white matter in Fig. 1c (yellow arrows). Figure 2 shows the left posterior angioma of Fig. 1, magnified and presented in normal and inverse grey scale. The tortuous vascular structure of the angioma is clearly seen. The origin of the enhancing rim may be related to the T1 hyperintense perilesional signal intensity observed previously in the presence of extravascular leakage of red blood cells and plasma during edema formation [6]. Inverse grey scale presentation appears to improve visualization. A brain stem cavernous angioma acquired at 3T is shown in Fig. 3. Here again, the angioma is characterized by hyperintense signal on the high resolution SGM map (Fig. 3b), while significant variations of the susceptibility gradient within the angioma can be observed (red arrows).

Discussion and Conclusion High resolution susceptibility gradient maps were computed to localize and characterize anatomical areas that, due to their local physiology, create local magnetic field perturbations. Cavernous angiomas are filled with blood at different stages, from very old (hemosiderin) to very fresh, which induces variations in the local magnetic susceptibility. Hence, the varying positive contrast signal that could be observed within the lesions due to the improved resolution may be an indication of the age of the angioma. Overall, in comparison to other susceptibility based techniques [2, 7], the method applied in this work does not require additional measurement time nor a priori knowledge about the observed susceptibility. This preliminary study shows the potential utility of positive contrast imaging for the visualization of localized vascular abnormalities at both 1.5T and 3.0T. Further investigation to determine its use as a routine imaging protocol should be pursued.

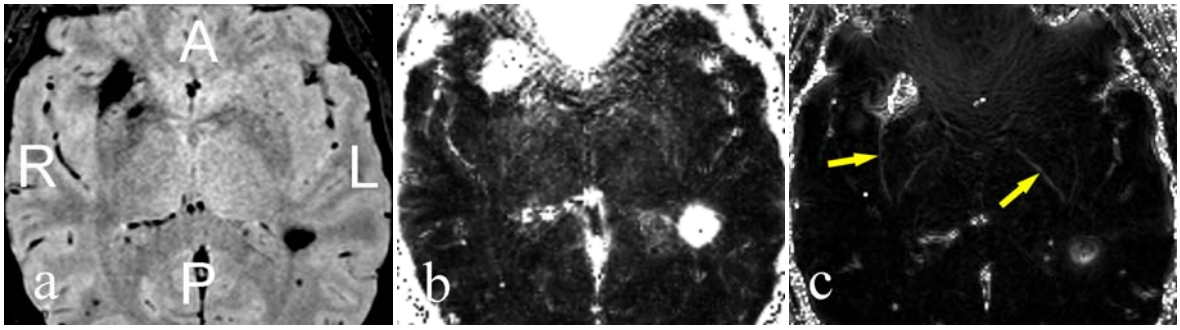

Fig. 1: Patient with multiple cavernous angiomas imaged at 1.5T. a: 3D PRESTO modulus image. b: low resolution positive contrast image. c: high resolution positive contrast image. Note the increased detail seen within the angiomas as well as the outline of the putamen in image c (yellow arrows).

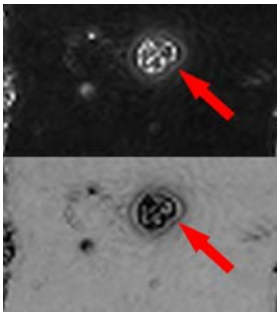

Fig. 2: Magnified view of the left posterior angioma of Fig. 1 from an adjacent slice shown in normal (top) and inverse (bottom) grey scales. Note the enhancing rim and structure within the angioma (red arrows).

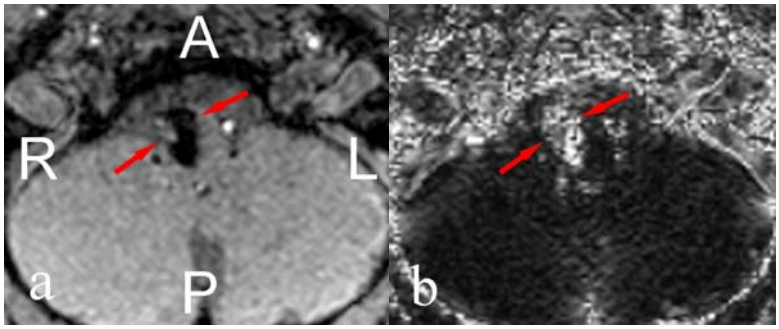

Fig. 3: Patient with brain stem cavernous angiomas imaged at 3.0T. a: 3D FFE modulus image. b: high resolution positive contrast image showing significant variations of the susceptibility gradient within the angioma (red arrows).

References [1] S. Posse, MRM, 25:12–29 (1992) [2] C. Bakker et al, MRM, 55:92-97 (2006). [3] H. Dahnke et al, ISMRM , #361 (2006) [4] H. Dahnke et al, MRM, 60: 595-603 (2008) [5] H. Dahnke et al, ISMRM, #1513 (2008). [6] T. J. Yun et al, AJNR, 29:494-500 (2008). [7] E. Haacke et al, MRM 52:612-628 (2004).